Resilient Structures and Sustainable Construction
Edited by Pellicer, E., Adam, J. M., Yepes, V., and Singh, A.

ISBN: 978-0-9960437-4-8

NUMERICAL ANALYSIS OF CONCRETE BEAM REINFORCED WITH GLASS FIBER REINFORCED POLYMER BARS

OSAMA A. MOHAMED and RANIA KHATTAB

College of Engineering, Abu Dhabi University, Abu Dhabi, United Arab Emirates

The use of fiber reinforced polymer (FRP) bars to reinforce concrete beams has received significant attention in the past decade due to their corrosion resistance, high tensile strength, and excellent non-magnetic properties. Glass FRP (GFRP) reinforcing bars have gained popularity due to the relatively lower cost compared to carbon FRP (CFRP) bars. In this study, sixteen concrete beam finite element models were created using the finite element computer program ANSYS to perform linear and non-linear analyses. Twelve beams were longitudinally reinforced with GFRP bars, while the remaining four beams were reinforced with conventional steel bars as control specimens. In terms of mechanical properties, FRP reinforcing bars have lower modulus of elasticity compared to conventional reinforcing steel and remain linear elastic up to failure. This leads to lack of plasticity and a brittle failure of beams reinforced with FRP bars. The objective of this study is to investigate flexural behavior of concrete beams reinforced with GFRP reinforcing bars. Some of the parameters incorporated in the numerical analysis include longitudinal reinforcement ratio and compressive strength of concrete, both of which affect the flexural capacity of beams. It is shown in this study that replacement of traditional reinforcing steel reinforced bars by GFRP bars significantly decreases mid-span deflection and increases ultimate load. The strain distribution along GFRP longitudinal reinforcing bars is totally different from that of traditional steel bars.

Keywords: GFRP bars, Steel bars, Flexure, Deflection, Ductility, Finite element.

1 INTRODUCTION

The use of FRP composite materials gained popularity in many parts of the world for retrofit of existing structures and potentially sustainable design of new structures. The movement to design with sustainable materials such FRP bars follows the evolution of retrofitting with sustainable FRP materials (Mohamed and Khattab 2016a) and (Mohamed and Khattab 2016b). FRP composites offer numerous advantages over conventional reinforcing steel including higher strength, higher stiffness, non-corrosive nature, and lower weight. FRP composites available for structural engineering applications at the present time are made of carbon, glass, and aramid. FRP composite bars that are commonly made from these three types of fibers used as internal reinforcement of concrete are referred to CFRP, GFRP, and AFRP bars, respectively. Guidelines for the design and construction of structural concrete reinforced with FRP bars are specified by ACI Committee 440 (2015). Studies conducted by various researchers confirmed that flexural capacity of concrete members reinforced with FRP bars can be calculated based on assumptions similar to those made for concrete members reinforced with steel bars (Nanni 1993) and

(GangaRao *et al*. 1997). Harajli and Abouniaj (2010) stated that the surface of the FRP bars is weaker and softer than that of steel bars, as a result, it is the surface of the FRP bar that may rupture instead of concrete, especially, at higher concrete strengths. Therefore, ribbed FRP bars are favored over threaded, wrapped, or spirally wrapped FRP bars. Table 1 summarizes the typical mechanical tensile properties of FRP bars compared to steel reinforcement.

Table 1. Typical tensile properties of steel and FRP reinforcing bars (ACI 440.1R-15 2015).

	Steel	**CFRP**	**GFRP**	**AFRP**
Nominal yield stress (MPa)	276 to 517	N/A	N/A	N/A
Tensile strength (MPa)	483 to 1600	600-3690	483 to 690	1720 to 2540
Elastic Modulus (GPa)	200	120-580	35 to 51	41 to 125
Yield strain (%)	0.14 to 0.25	N/A	N/A	N/A
Rupture Strain (%)	6.0 to 12.0	0.5 to 1.7	1.2 to 3.1	1.9 to 4.4

Due to the benefits discussed earlier in this paper, extensive theoretical and experimental research has been performed in the past few years to examine the behavior of concrete beams reinforced with FRP bars. Many studies emphasized deflection characteristics and flexural ductility of beams reinforced with FRP bars. Habeeb and Ashour (2008) presented a set of experimental investigations on flexural behavior of continuous concrete beams reinforced with GFRP bars. El-Mogy *et al*. (2010) tested four two-span continuous beams, including two beams reinforced with GFRP bars, one beam reinforced with CFRP bars, and one beam reinforced with conventional steel bars. Santos *et al*. (2013) conducted an experimental and numerical study on ductility and moment redistribution in continuous GFRP reinforced concrete T-shaped beams.

2 FLEXURAL CAPACITY OF GFRP REINFORCED CONCRETE BEAMS

Chaallal and Benmokrane (1995) used Eq. (1) to determine the ultimate flexural strength, Mu, of beams reinforced with GFRP bars.

$$M_u = \phi A_f f_y \left(d - a/2\right) \tag{1}$$

where,

ø = 0.75 is flexural strength reduction factor proposed based on a probabilistic approach by Benmokrane *et al*. (1996b) for beams reinforced with GFRP bars.

f_y, is taken as the ultimate tensile strength of the GFRP reinforcement bar.

d is the effective depth of the beam section.

Alsayed *et al*. (2000) proposed Eq. (2) to find the flexural strength of the GFRP reinforced concrete based on the ACI 318 (1992). This equation ensures beam failure is controlled by tensile failure of the reinforcing bars.

$$M_n = A_p f_{py} d\left[1 - 0.59\rho_p\left(f_{py}/f_c'\right)\right] \tag{2}$$

In Eq. (2), the pseudo yield strength, f_{py}, of the GFRP bars is assumed to occur at 0.67 of the ultimate tensile strength, f_{pu}, and A_p is the area of GFRP reinforcement.

The nominal moment strength of the GFRP reinforced concrete member that fails by compression of concrete is calculated from the Eq. (3).

$$M_n = A_p f_{ps}\left(d - a/2\right) \tag{3}$$

In compression-controlled failure, the tensile strain in the reinforcing bars, ε_{ps}, is related to the pseudo yield strain, ε_{py} by Eq. (4).

$$\varepsilon_{ps} = \left(\varepsilon_{cu}\left(d - c\right)/c\right) \tag{4}$$

In Eq. (4), ε_{cu} is the concrete strain at the extreme compression fiber and c is the distance from that fiber to the neutral axis.

In Eq. (2) and Eq. (3), the flexural strength reduction factor, ø, is considered as 0.9.

3 FINITE ELEMENT MODELLING

ANSYS computer program was used in this paper for the finite element modelling of concrete beam reinforced with GFRP bars. SOLID65 element is used to model plain concrete material with the capability of cracking in tension and crushing in compression. SOLID65 element is defined by eight nodes with three translational degrees of freedom at each node and is capable of representing plastic shrinkage and creep behaviors. The element material is assumed to be initially isotropic. Reinforcing steel and GFRP bars were represented by LINK8 element, which is a uniaxial tension-compression member that includes nonlinear material properties. LINK8 consists of two nodes with three degree of freedom at each one and the material behavior is assumed to be elastic-perfectly plastic. Appropriate load transfer to Link8 element occurs when it is located between two or more SOLID65 elements, otherwise, the forces would only be transferred at the nodes of SOLID65.

A smeared crack model is implemented by ANSYS program where a shear transfer coefficient, $\beta_{t,}$ represents the shear strength reduction factor for subsequent loads that induce sliding shear across the crack face. When the crack closes, all compressive stresses normal to the crack plane are transmitted and only a shear reduction factor, β_c. Typical shear transfer coefficients range from zero, representing a smooth crack, to one, representing a rough crack. In the present analysis, β_t was taken as 0.1 and β_c was taken as 0.8.

4 DESCRIPTION OF THE MODELS

In this paper, sixteen reinforced concrete beams were modelled and analysed using ANSYS software. Four of the beams were longitudinally reinforced with conventional steel bars for benchmarking and 12 beams were longitudinal reinforced with GFRP bars. The mean reinforcement ratio, ρ_s, varied from 0.56% to 1.19%. To ensure flexural failure, shear failure is eliminated by reinforcing the beam with eight mm diameter shear ties spaced at 150 mm. Beam dimensions and reinforcement details are shown in Figure 1. Three types of concrete were modelled with compressive strength, f_c', equal to 30 MPa, 40 MPa, and 50 MPa.

As shown in Table 2, each set of four beams was modelled with one specific concrete strength. The four beams that are reinforced with conventional steel bars (SB1 to SB4) are modelled with only 30 MPa concrete for comparison with the four beams reinforced with GFRP (GFB1 to GFB4) and modelled with the same 30 MPa concrete strength.

Table 2 also shows that there are four beams modelled with each reinforcement ratio. For example, there are four beams reinforced with 0.56%, and four beams with reinforcement ratio of 0.79%.

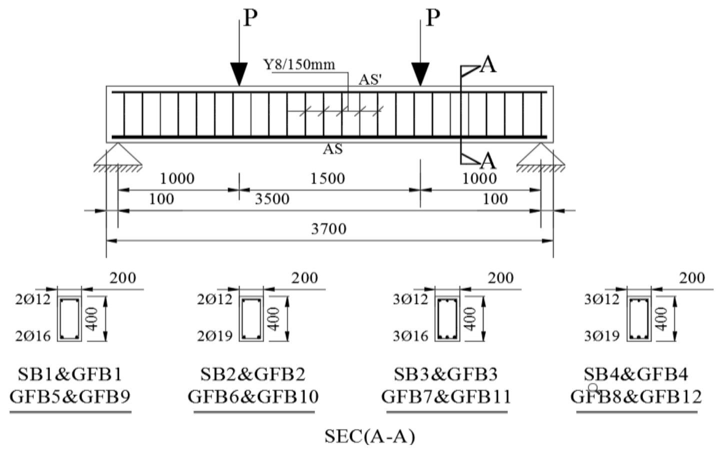

Figure 1. Beams details and properties.

Table 2. Specifications of beams.

Beam	**Reinforcing bar**	**Diameter of bar (mm)**	**No. of bars**	A_s (mm^2)	ρ_s **(%)**	f_c', *(Mpa)*
SB1	Steel	16	2	402.10	0.56	30
SB2	Steel	19	2	567.10	0.79	30
SB3	Steel	16	3	603.20	0.84	30
SB4	Steel	19	3	850.60	1.19	30
GFB1	GFRP	16	2	402.10	0.56	30
GFB2	GFRP	19	2	508.90	0.79	30
GFB3	GFRP	16	3	603.20	0.84	30
GFB4	GFRP	19	3	763.40	1.19	30
GFB5	GFRP	16	2	402.10	0.56	40
GFB6	GFRP	18	2	508.90	0.79	40
GFB7	GFRP	16	3	603.20	0.84	40
GFB8	GFRP	19	3	763.40	1.19	40
GFB9	GFRP	16	2	402.10	0.56	50
GFB10	GFRP	19	2	508.90	0.79	50
GFB11	GFRP	16	3	603.20	0.84	50
GFB12	GFRP	19	3	763.40	1.19	50

Table 3 shows the tensile strength, modulus of elasticity, and ultimate strain for GFRP and steel bars modelled in this study. The 8-mm diameter steel bar is used for shear reinforcement. The tensile strength of 16-mm diameter GFRP bars is slighter higher than the 19-mm bars, but doesn't affect the main conclusions in this study.

Table 3. Properties of GFRP and steel reinforcing bars.

	Diameter (mm)	**Tensile Strength (MPa)**	**Modulus of Elasticity (GPa)**	**Ultimate Strain**
GFRP	16	724	46	0.016
GFRP	19	690	46	0.015
Steel	16	512	200	0.0026
Steel	12	512	200	0.0026
Steel	19	512	200	0.0026
Steel	8	440	162	0.0028

5 RESULTS

Figure 2 shows the load versus mid-span defection for beams reinforced with various ratios of GFRP bars. The expected bilinear response of beams reinforced with FRP bars is evident for all reinforcement ratios. At can be seen that for any particular value of mid-span deflection, increasing the reinforcement ratio increases the ultimate load. Similarly, ultimate load increases by increasing the compressive strength of concrete.

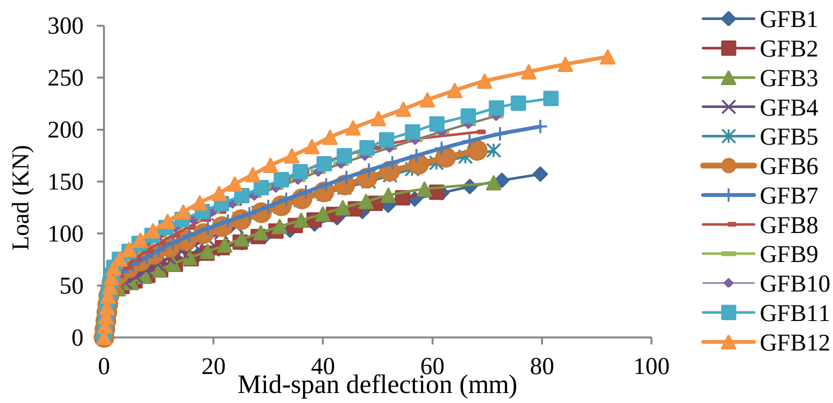

Figure 2. Load versus mid-span deflection for various GFRP reinforcements and concrete strengths.

Table 4. Specifications of beams.

Beam	Ultimate Load, Pu (KN)	Max. Deflection (mm)	Ultimate tensile force bars (KN)	Ultimate Concrete Compressive stress (N/mm^2)
SB1	115.60	42.20	80.00	12.70
SB2	129.50	46.27	97.43	13.81
SB3	140.00	31.46	85.30	15.75
SB4	156.97	40.25	98.89	17.24
GFB1	157.20	79.70	117.92	18.38
GFB2	160.40	84.33	114.27	19.69
GFB3	173.80	89.85	101.20	21.82
GFB4	184.66	95.83	115.10	25.76
GFB5	180.00	71.18	108.52	22.08
GFB6	187.00	78.17	120.90	23.08
GFB7	203.00	79.70	117.00	25.58
GFB8	210.56	89.33	135.45	30.96
GFB9	213.15	71.62	110.31	29.31
GFB10	220.77	77.52	129.19	31.22
GFB11	230.55	81.64	112.25	33.27
GFB12	270.45	92.02	142.75	36.44

Table 4 summarizes the output data for all of the beams modelled in this study. It can be observed from Table 4 that the replacement of steel reinforcement for each of the tested ratios with GFRP bars increases the ultimate load for 30 MPa concrete compressive strength by as much as 36%. Similarly, the maximum deflection at failure load increases with increase in GFRP reinforcement ratio that replaces conventional steel.

Furthermore, the replacement of steel reinforcement with GFRP bars increases the ultimate compressive concrete stress by approximate 44.7%, 42.6%, 38.54%, and 49.4% at reinforcement ratios of 0.56, 0.79, 0.84, and 1.19 respectively.

6 SUMMARY AND CONCLUDING REMARKS

The numerical analysis on four steel reinforced beams and twelve GFRP reinforce beams have been presented and discussed in this paper. All GFRP reinforced beams exhibited the traditional bilinear behavior until failure, due to linear response of GFRP reinforcement bars. In addition, the failure of GFRP reinforced beams took place at large displacements compared to steel reinforced beams for the same reinforcement ratio and concrete strength. The ultimate moment capacity for the beam specimens is considerably improved with the use of GFRP bars compared to steel reinforced concrete beams with the same reinforcement ratio and concrete strength. The addition of GFRP increased the load at first-cracking and the ultimate flexural strength.

Acknowledgement

The authors gratefully acknowledge the financial support of the Office of Research and Sponsored Programs (ORSP) and the Center on Sustainable Built Environment at Abu Dhabi University under grants number 19300074 and 19300105.

References

ACI Committee 440, Guide for the Design and Construction of Structural Concrete Reinforced with Fiber-Reinforced Polymer (FRP) Bars, ACI 440.1R-15, American Concrete Institute, USA, 2015.

Alsayed, S. H., Al-Salloum, Y.A., and Almusallam, T.H., Performance of glass fiber reinforced plastic bars as a reinforcing material for concrete structures, *Composites: Part B-engineering*, Elsevier, V. 31, 555-567, 2000.

ANSYS Mechanical APDL Manual Set, Release 14.5, ANSYS, Inc., USA,2 012

Benmokrane, B., Chaallal, O., and Masmoudi, R., Flexural Response of Concrete Beams Reinforced with FRP Reinforcing Bars, *ACI Structural Journal*, 91(2), 46-55, 1996b

Challal, O., and Benmokrane, B., Fiber-reinforced plastic reinforcement bars for concrete Applications, *Composites Part B: Engineering*, Elsevier, V.27, pp. 245-252, 1995.

El-Mogy, M., El-Ragaby, A., and El-Salakawy, E., Flexural behavior of continuous FRP-reinforced concrete beams, *Journal of Composites for Construction*, ASCE, 14(6), 669-680, 2010.

GangaRao, H. V. S., and Vijay, P. V., Design of Concrete Members Reinforced with GFRP Bars, *Proceedings of the Third International Symposium on Non- Metallic (FRP) Reinforcement for Concrete Structures (FRPRCS-3),* Japan Concrete Institute, Tokyo, Vol.1, 143-150,1997.

Habeeb, M. N. and Ashour A. F., Flexural behavior of continuous GFRP reinforced concrete beams, *Journal of Composites for Construction,* ASCE, 12(2), 115-124, 2008.

Harajli, M., and Abouniaj, M., Bond Performance of GFRP Bars in Tension: Experimental Evaluation and Assessment of ACI 440 Guidelines", *Journal of Composites for Construction*, ASCE, 14(6), 659-668, 2010.

Mohamed, O. A. and Khattab, R., Numerical Analysis of Reinforced Concrete Beam Strengthened with CFRP and GRP Laminates, *Key Engineering Materials*, vol. 707, 51-59, 2016a.

Mohamed, O. A. and Khattab, R., Bond-slip Modelling of FRP Sheets Externally Bonded to Concrete Beam, *Procedia Engineering*, Elsevier , vol. 161c –,833-838, 2016b.

Nanni, A., Flexural behavior and design of RC members using FRP reinforcement, *Journal of Structural Engineering*, ASCE, 119(11), 3344–3359, 1993.

Santos, P., Laranja, G., Franca P. M., and Correia J. R., Ductility and moment redistribution capacity of multi-span T-section concrete beams reinforced with GFRP bars, *Construction and Building Materials*, Elsevier, vol. 49, 949-961, 2013.